Journal of Materials Chemistry A

Nano-composite structural Ni-Sn alloy anode for high performance and durability of direct methane-fueled SOFCs

Journal:	*Journal of Materials Chemistry A*
Manuscript ID:	TA-ART-11-2014-006037.R1
Article Type:	Paper
Date Submitted by the Author:	04-Apr-2015
Complete List of Authors:	Myung, Jaeha; University of St Andrews, Chemistry; Yonsei University, Department of Materials Science and Engineering Kim, Sun-Dong; Korea Institute of Energy Research, Energy Materials Center Shin, Tae Ho; University of St Andrews, Chemistry Lee, Daehee; Yonsei University, Department of Materials Science and Engineering Irvine, John T.S.; University of St Andrews, Chemistry Moon, Jooho; Yonsei University, Department of Materials Science and Engineering Hyun, Sang-Hoon; Yonsei University, Department of Materials Science and Engineering

Journal Name

RSCPublishing

ARTICLE

Nano-composite structural Ni-Sn alloy anode for high performance and durability of direct methane-fueled SOFCs

Cite this: DOI: 10.1039/x0xx00000x

Received 00th January 2012,
Accepted 00th January 2012

DOI: 10.1039/x0xx00000x

www.rsc.org/

Jae-ha Myung[1,3], Sun-Dong Kim[2], Tae Ho Shin[3], Daehee Lee[1], John T.S. Irvine[3], Jooho Moon[1] and Sang-Hoon Hyun[1,*]

Ni-based cermets have commonly been used as the anode material with good catalyst properties for hydrocarbon fuels. However, carbon deposition can be occurred from the non-ideal electrochemical reaction of hydrocarbon fuel and the structural limitation resulting from the unsymmetrical Ni-based anode-supported single cells. This critical problem leads to loss of cell performance and poor long-term stability of solid oxide fuel cells (SOFCs). Our designed anode material, the extreme small amount (0.5 wt%) of Sn catalyst incorporated onto Ni and nano-composite structure, were employed not only to prevent the carbon deposition in oxygen deficient areas found for unsymmetrical cells, also increase the cell performance due to the excellent microstructure. The nano-composite Sn doped Ni-GDC cells showed 0.93 Wcm^{-2} with stable operation in dry methane at 650 ^{o}C.

Introduction

Solid oxide fuel cells (SOFCs) are high attractive for next generation energy systems directly converting chemical energy into electrical energy with high efficiency and low emissions.[1, 2] They also provide outstanding fuel flexibility without the use of external reformers and thus the direct utilization of hydrocarbons is one of the most important issues concerning SOFCs.[3-5] Among the various utilizable fuels, methane has been attractive as one of the effective fuels due to its abundant supply, low-cost and its compatibility with the current well-developed gas distribution infrastructure. However, the use of methane fuel for practical SOFC stacks of large scale systems has been limited because of several challenging issues such as low anode reliability; deactivation and fracture of cell or stack by carbon formation in Ni-based conventional anode under severe operating conditions.[6, 7] Therefore, advanced anodes for Ni-base anode with a reliable metal such as Cu-based metals or oxide anodes have recently been investigated to prevent carbon coking.[8-12] Perovskite-structured anode materials such as $(La_{0.75}Sr_{0.25})Cr_{0.5}Mn_{0.5}O_3$ (LSCM) showed comparable performance to Ni/YSZ cermet anodes with high efficiency and high resistance to carbon deposition when using hydrocarbon fuels.[13] A $Ce_{0.6}Mn_{0.3}Fe_{0.1}O_2$-$La_{0.6}Sr_{0.4}Fe_{0.9}Mn_{0.1}O_3$ anode has been reported to deliver 1 Wcm^{-2} power density with propane and butane fuels resulting from high catalytic activity in relation to direct hydrocarbon oxidation.[14] However, the power densities of these anode oxides are still lower than that of the conventional Ni-based anode when it is using methane fuel at lower temperature because of insufficient electrical conductivity and catalytic activity with respect to methane. The Ni based anodes obviously have high catalytic activity for methane reforming in comparison with oxide anodes. However, the oxide anodes are still required to optimize the compositions and microstructures for high redox stability and tolerance of carbon deposition in order to commercialize direct methane fueled SOFCs. In our previous work, the nano-surface modified anode with nano-composite powder, NiO/GDC-GDC (n-NGG), showed the effects on the tolerance of carbon deposition and advancement of fuel oxidation with large three phase boundaries (TPBs), which increase performance and long-term stability.[15] However, the carbon deposition partially occurs in areas where oxygen ions were not supplied to the anode in the case of large scale cells due to the unsymmetrical cells comprising different active areas for electrodes and inconsistent distributions of methane (as shown in Fig. 1). In particular, carbon is deposited on the edge of stack components due to the lack of the oxygen ions from an unsymmetrical cathode coating layer which was similarly observed in our large scale SOFC stack test. Thus far, catalyst additives are mainly used to avoid carbon deposition on the anode surface; other researchers have been researching catalysts such as Ru, Au, and Rh doped Ni-based cermet and Cu-based anode replaced of Ni, but they could not achieve performances comparable to Ni-based anode supported cells even though they could suppress carbon deposition for methane fuel.[16-20] Among various additives, Sn catalyst has recently been introduced as a promoter for transfer of solid carbon and kinetic activators for the electrochemical oxidation of carbon in direct carbon fuel cells (DCFCs).[21] Sn-Ni alloys have a higher inclination to oxidize carbon and computational models suggest that they are more carbon-tolerant than Ni, however performance has not exceeded 0.5 Wcm^{-2} at intermediate temperatures due to the simple doping of the alloy on natural materials.[22-24]

Thus, in this work, we have chosen Sn doped Ni-GDC anode with an optimized nano-composite anode to enhance its effects on tolerance of carbon deposition by carbon oxidation catalytic activity of Sn and the large TPBs of nano-composite structure. The abbreviation and the nature of the anode materials (NG, SNG, n-NGG and n-SNGG) in this study are explained in the Table 1. We improved the durability and power density when using methane fuel at 650 ^{o}C on a practical SOFC stack sized cell system. Furthermore, the various effects of combining Sn and our unique nano-composite structure to delay carbon diffusion and C-C bond formation by destabilising C-Ni bonding, acts as an anti-sintering aid leading to retained porosity.

Table 1. Summarized charactersitics of as-preapred anode materials

Sample	Characteristics
Ni-GDC (NG)	Mechanical mixutre of Ni and GDC cermet anode
Sn doped Ni-GDC (SNG)	Mechanical mixutre of Sn doped Ni and GDC cermet anode
Ni/GDC-GDC (n-NGG)	Nano sized Ni and GDC conjugated on a core GDC nano-composite anode
Sn doped Ni/GDC-GDC (n-SNGG)	Sn doped nano sized Ni and GDC conjugated on a core GDC nano-composite anode

Experimental

Powder Preparation. NiO/GDC-GDC powder was synthesized using the Pechini process. The composition ratio of the embedded Ni metal and GDC, and core GDC as the reduced anode was 40:30:30 vol%. The precursors of $Ni(NO_3)_2$•$6H_2O$ (Junsei Chemical Co., 97.0%), GdN_3O_9•$6H_2O$ (Aldrich, 99.9%), and $Ce(NO_3)_3$•$6H_2O$ (Kanto Chemical Co., 99.99%) were stoichiometrically added to DI water and heated to 40 °C. Next, citric acid (Junsei Chemical Co., 99.5%) and ethylene glycol (Ducksan Pure Chemical, 99.5%) with molar ration of 1:2.5 were added to this solution as complexation and polymerization agents, respectively, at 60 ^{o}C. Then, GDC powder (Rhodia, ULSA grade) was added as core particles to the aqueous solution. The polymeric solution was condensed at 180 °C for 4 hours and ash-colored intermediates were obtained. Finally, NiO/GDC-GDC nano-composite powders were obtained after calcination at 600 °C for 2 hours. The Sn (0-1 wt% of Ni) was doped on commercial NiO powders (J.T. Baker) and the synthesized NiO/GDC-GDC powders by using the incipient wetness technique. $SnCl_2$•$2H_2O$ (Aldrich) was dissolved in a corresponding amount (500ml) of ethanol and then synthesized 20g of NiO/GDC-GDC (Rhodia, ULSA grade) or NiO powder was added into the solution under stirring and heating. The dried powder was calcinated at 600 ^{o}C for 2 hours.

Dry methane Flow Test. The anode samples were reduced in a H_2 atmosphere at 650 ^{o}C for 3 hours and the reduced samples were weighed. Then, the samples were heated up to 600~900 ^{o}C in N_2 atmosphere and heated at 600~900 ^{o}C for 30 minutes in CH_4 atmosphere. Finally, The amount of deposited carbon for different amounts of Sn (0-1 wt%) in the NiO/GDC-GDC anode powder were weighed after cooling in N_2 atmosphere. The out gases from the methane flow test conducting at 900 ^{o}C were also analysed by gas chromatography.

.

Fabrication of single cells. Anode supported cells consisting of Ni-GDC (t = 1mm, Area = 5.3 cm^2) | GDC (t = 12 μm) | LSCF-GDC (t = 20 μm, Area = 1.0 cm^2) were fabricated for electrochemical characterisation. The Ni-GDC (10 wt% of carbon black) anode supports were fabricated by a uni-axial pressing method and burn-out at 1150 ^{o}C for 3 hours. GDC electrolyte was deposited by dip-coating method and sintering at 1350 ^{o}C for 3 hours. The LSCF-GDC cathodes (LSCF:GDC = 50:50 wt%) was fabricated by screen printing with a paste of LSCF (Fuel Cell Materials Co., Lewis Center, OH, USA) and GDC powders followed by sintering at and 1000 ^{o}C for 2 hours.

SOFC Cell Test. The performances of the cells were analyzed at 650 ^{o}C in reactive gases of H_2 (50 $ccmin^{-1}$ at standard ambient temperature and pressure) or dry methane (15 $ccmin^{-1}$ at standard ambient temperature and pressure) without any balanced gas at the anode and air (500 $ccmin^{-1}$ at standard ambient temperature and pressure) at the cathode. The I-V curves and durability were measured using a multi-functional electronic load module (3315D, Taiwan). AC impedance measurements were carried out using a Solatron 1260 frequency analyser and a Solatron 1287 interface.

Other characterisations. The pore size distribution of anodes which were fabricated by the same heat-treatment as cell fabrication and reduced in H_2 atmosphere at 650 ^{o}C were analysed by a mercury porosimeter (Micromeritics). Scanning electron microscope (SEM, JEOL) and transmission electron microscope (TEM, JEOL) were used for analysing the elemental distribution and structure of powders synthesized. For ex-situ surface characterisation, the cells were cooled to room temperature under N_2 purging. X-ray photoelectron spectroscopy (XPS, K-alpha, Thermo Fisher Scientific Inc.) was conducted for analysis of Ni oxidation of Ni-GDC anode. Carbon deposition from the single cells after operating with CH_4 fuel were analysed by temperature programmed oxidation (TPO) and SEM.

Results and discussion

The presence of Ni in the fuel environment enables hydrocarbon fuels to be reformed directly on the anode, while oxygen ions are constantly transported from the cathode to the anode through the electrolyte under load conditions.

SOFCs are also considered to be chemical reactors, producing a variety of useful chemicals depending on the fuel mixture and operating mode, which is known as direct electrochemical oxidation.

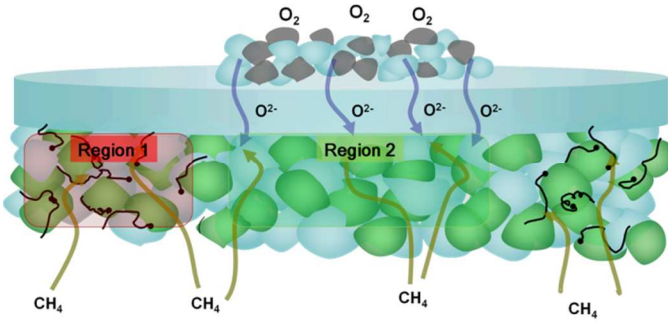

Fig. 1 Schematic illustration of the reaction mechanisms depending on the anode regions of the direct methane utilized SOFCs.

This direct electrochemical oxidation of fuels at the anode is highly exothermic and is the opposite of the reforming reaction, which is full oxidation, as shown in equation (1).

$$CH_4 + 4O^{2-} \rightarrow CO_2 + 2H_2O + 8e^- \quad (1)$$

The direct electrochemical oxidation of methane fuel is a 100% Faradic-coupled reaction, as hydrocarbon fuel is oxidized with oxygen ions from the cathode and transported through the dense electrolyte as the region 2 in Fig. 1

The deposited carbons can be also oxidized, as shown in equation (2) and (3)

$$C + 2O^{2-} \rightarrow CO_2 + 4e^- \quad (2)$$

$$C + O^{2-} \rightarrow CO + 2e^- \quad (3)$$

These carbon oxidation reactions require the enough oxygen ions and the lower C-O bonding energy than the C-C bonding.

However, these reactions may not go to completion because of the non-ideal electrochemical reaction or excess amount of methane and the structural limitation resulting from the unsymmetrical anode-supported single cells consisting of the smaller area of the cathode than the anode support as the region 1 in Fig. 1. This leads to carbon deposition following equations (4) and (5).

$$2CO \rightarrow CO_2 + C \quad (4)$$

$$CH_4 \rightarrow 2H_2 + C \quad (5)$$

Filamentatious carbon or graphitic carbon were formed by these pyrolysis and Boudouard reactions , leading to internal stress and destruction of the anode support.

The doping of small quantities of another metal on the surface of Ni particles can protect the catalytic activity against the formation of carbon. In this work, Sn dissolved Ni cerments, were demonstrated to be higher carbon tolerant than monometallic Ni in methane by lowering the activation energy of the C-O bond.

One of the critical factors in the application of non-coking SOFC anodes is the uniformity of catalyst on the anode structure because the catalyst distribution is strongly relative with surface activity area and TPBs.[15, 25, 26] As the results of the TEM and EDS analysis of Sn-doped NiO and NiO/GDC-GDC (n-SNGG) show (Fig. 2), Sn doping on commercial NiO showed inhomogeneous distributions and coarsening, otherwise, the Sn was homogeneously covered on the synthesized n-NGG nano-composite powder and all comprising elements, Ce and Ni were homogeneously distributed as well. It is because the Sn doped onto the NiO nano particles embedding on core GDC, which limits the metal coarsening and segregation during the firing process.

a

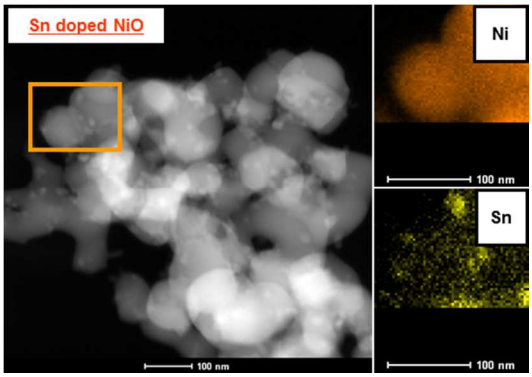

b

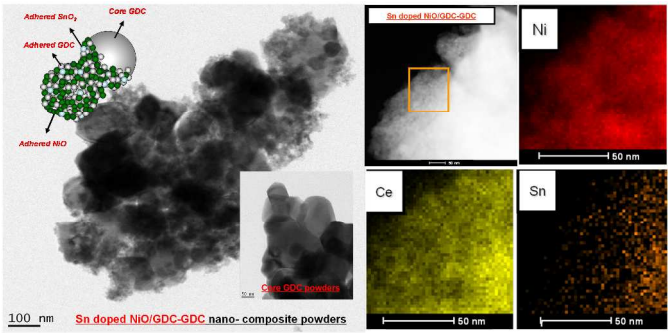

Fig. 2 TEM image and EDS analysis of the Sn doped (a) NiO and (b) NiO/GDC-GDC nano-composite powders.

The n-SNGG can lead to higher electrical conductivity, mechanical strength and higher power density via improving the surface area, metal connectivity and the oxide sinter-ability.

Basically, the SOFC anodes should have the specific microstructure of smaller pore size and higher porosity for large TPBs, which strongly influence the performance and durability improving mass transfer, electrical/ionic conductivity and mechanical strength of the SOFC anode.[27-29] Owing to the addition of an extremely small amount of Sn to the embedded Ni of n-NGG, the microstructures of n-SNGG anode substrates could be vastly improved to average pore size and porosity which is strongly relative to TPB in comparing to the conventional NG. The samples, sintered and reduced at 1,350 ^{o}C and 650 ^{o}C, respectively, clearly show that Sn doping and nano-composite anode retain the suitable microstructure with fine pore-size and high porosity after high firing temperature (Fig. S1, ESI†).

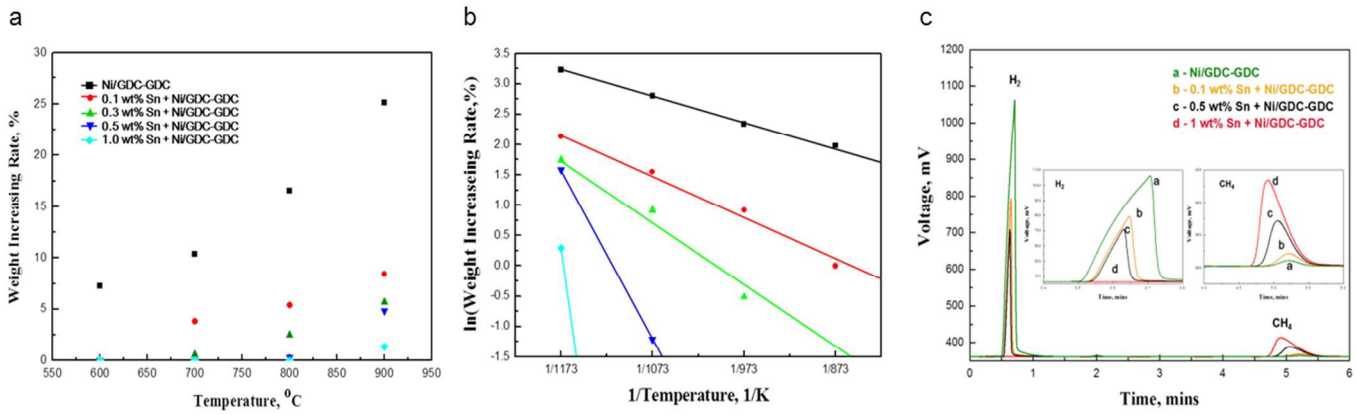

Fig 3. (a) Weight increasing rate by carbon deposition as functions of temperature and Sn doping contents from 600~900 ^{o}C and transformed to (b) Arrhenius plots, and (c) gas chromatography results of the methane pyrolysis reaction on anode powders at 900 ^{o}C.

The Sn doping on NG anode, leads to increase the porosity from 36.30 % to 43.18% and slightly decrease an average pore size from ~550 to ~530 nm. Moreover, in the case of Sn doping on nano-composite anode, the porosity of the n-SNNG anode improved from 46.62 % to 50.13 % with an average pore size of ~420 nm to ~410 nm compared to those of the n-NGG anode. These results are caused by the agglomeration inhibition of nano-composite structure that the embedded nano Ni particles between GDC particles on a core GDC. According to Zhaoying et al., Sn is also demonstrated for improving the dispersion of Ni, and retarded the sintering of Ni.[30] This n-SNGG anode with the enlarged TPBs and non-agglomerated materials strongly affects the cell performance and durability, as described later in this paper.

The other effect of Sn-doped NiO on SOFC anodes is to suppress the carbon deposition produced from the methane pyrolysis which occurs on the Ni-based anode due to lack of oxygen ions as a thermochemical reaction. A dry methane flow test was conducted with these powders at various temperatures to estimate approximately the activation energies of the methane pyrolysis reaction. Fig. 3a shows that a higher Sn content on n-NGG leads to less carbon deposition at each temperature. The results were converted to an Arrhenius plot in Fig. 3b, where the slope represents the activation energy of the reaction. It is demonstrated that as more Sn catalyst is doped on the anode, the activation energy of the methane pyrolysis increases and the carbon deposition rate is reduced. Gas chromatography was also used to determine the pyrolysis reaction rate by analysing the gases produced from the methane flow tests and the results are shown in Fig. 3c. The peaks at 0.5 and 5 min of retention time represent the amount of hydrogen and methane gas, respectively. If there is a more active methane pyrolysis reaction on the sample, these areas will decrease and result in increased carbon deposition.

The red line (1) represents 20 ccmin^{-1} of methane without sample and does not show the reformation to hydrogen gas and can be used as a control. The green line (2) corresponding to the n-NGG powder had the largest area representing the amount of hydrogen gas reformed by methane pyrolysis reaction. The methane conversion rate was reduced from 95 % to 67 % and 49 % by increasing Sn concentration for 0.5 and 1 wt% n-SNGG. It seemed that Sn can suppress the carbon deposition reaction by reducing activation energy for C-H bonding breaking from methane pyrolysis reaction on Ni.

Fig 4a and 4b show the performance and durability test results of the NG and SNG anode-supported cells operating in H_2 and CH_4 at 650 ^{o}C in the initial stage of measurements. The maximum power densities of the NG cell were 0.42 Wcm^{-2} with H_2 and 0.35 Wcm^{-2} with CH_4 with 1.5 hours of stable operation. Compared to this, the SNG cells showed power densities of 0.50 Wcm^{-2} with H_2 and 0.36 Wcm^{-2} with CH_4 over 250 hours of stabile operation. Carbon is mostly deposited on areas that are poorly supplied with oxygen ions, such as on the edge of the anode on an unsymmetrical cell and the anode surface away from TPBs. The deposited carbon can be analysed by temperature programmed oxidation (TPO) oxidizing the deposited carbon with a 5 % oxygen-helium mixture gas, while the reactor is heated with programmed temperature profile. The TPO results (Fig. 5) show that the SNG cells after 250 hours operation have much smaller area as 9.4 % compared to the NG cells after 1.5 hours of operation. The small amounts of Sn doped in the Ni showed a primary effect suppressing carbon deposition. The small amount of carbon on Sn doped Ni would be the beneficial side effect for improving the cell performance by increasing the electrical conductivity from bridging between metal particles and using electrochemical oxidation of the carbon as a fuel.

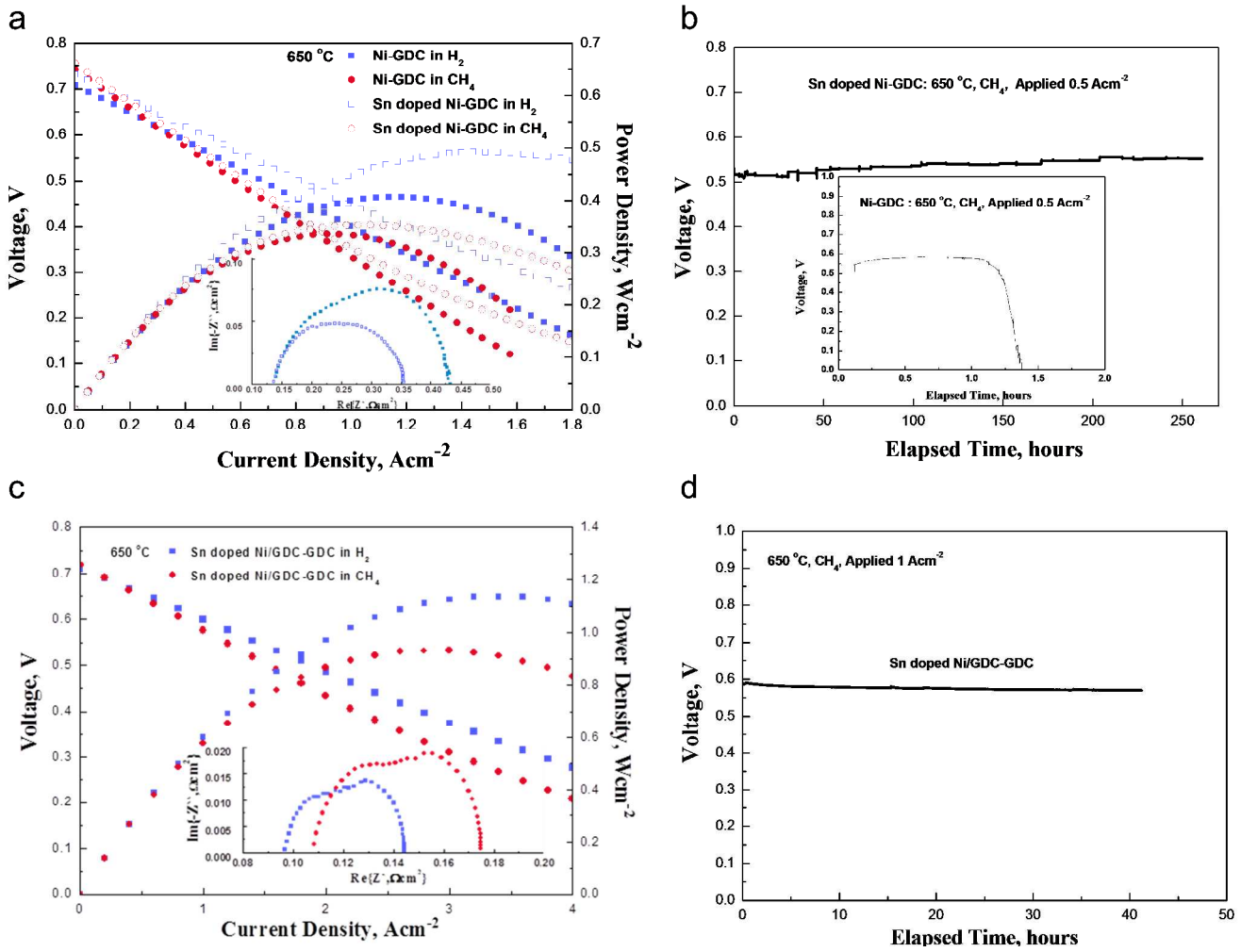

Fig 4. I-V curves and stability tests for (a-b) the conventional Ni-GDC anode-supported single cell (closed) and the 0.5 wt% Sn doped Ni-GDC anode-supported singlet cell (opened), (c-d) the 0.5 wt% Sn-doped Ni/GDC-GDC anode-supported single cells with H_2 (blue) and CH_4 (red) at 650 oC

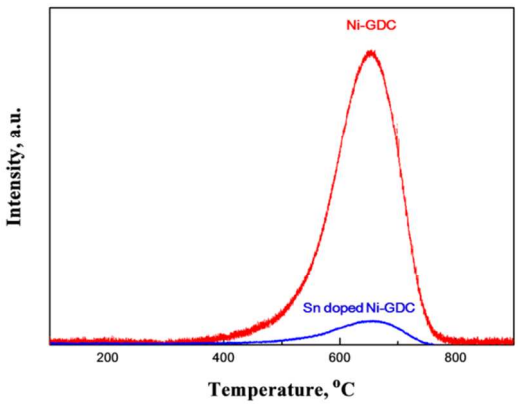

Fig 5. Temperature-programmed oxidation (TPO) results and the cross-sectional SEM images from (red) Ni-GDC and (blue) 0.5 wt% Sn-doped Ni-GDC single cells after their long-term stability tests with dry methane.

SEM images also showed that the SNG cells prevent carbon deposition, while filamentous carbon was deposited on the anode after the long-term stability test in the case of the conventional NG cell (Fig. S2a and S2b, ESI†). A further explanation is that the oxygen ions would prefer to be used for oxidizing the carbon than oxidizing Ni metal by lowering the overall activation barrier for the carbon oxidation (C-O bonding). This result leads to suppression of Ni oxidation and carbon deposition, also higher performances at low temperature in dry methane. Single cells made from the surface modified nano-composite powders were also tested for higher performances and stability with lower polarization resistance and extended TPBs in the anode.

The power densities of the 0.5 wt% SNGG cells were 1.13 Wcm^{-2} and 0.93 Wcm^{-2} with H_2 and CH_4, respectively, and the ohmic and polarization resistances were 0.097 Ωcm^2 and 0.047 Ωcm^2 with H_2 respectively, and 0.107 Ωcm^2 and 0.068 Ωcm^2 with CH_4 at 650 °C (Fig. 4c). The 0.5 wt% n-SNGG

cells could operate for over 40 hours without any degradation, as shown in Fig. 4d. The research groups studying Sn effects have mostly observed that an optimal amount of Sn doping on Ni is required to achieve the high catalytic activity for dry methane and suppress carbon deposition simultaneously.[30-32]The effect of Sn on preventing carbon deposition is also demonstrated with large scale anode-supported (Fig. S3 and S4, ESI†).

The development of large-scale cell or practical SOFC stack for direct utilization of dry methane require novel anode materials, innovative bi-polar plate, and the complex BOP for long-term stability at intermediated temperature. However, extremely small amount of Sn doping on Ni would be the one of the cost-effective core solutions to utilize directly hydrocarbon fuels.

Conclusions

We evaluated the effects of the extremely small amount of Sn on micro-structure and resistance to carbon deposition as well as the performance and durability with dry CH_4. The Sn was doped on conventional NiO powder and the surface modified powder by the simple incipient wetness method. The n-SNGG powder has better homogeneous distribution of Sn, because Sn is doped on the nano-sized NiO embedded on the core GDC. The microstructures of the anodes were considerably improved by the Sn catalyst which plays the role of coarsening inhibitor, resulting in higher porosity and smaller pore size. The maximum power density of the 0.5 wt% n-SNGG anode-supported cells were 1.12 Wcm^{-2} and 0.93 Wcm^{-2} with H_2 and CH_4 respectively at 650 ^oC, which are considerably improved comparing with the conventional Ni-GDC single cells.

Acknowledgements

This work was supported by the Seoul R&BD Program (CS070157). It was also partially supported by a National Research Foundation (NRF) of Korea grant funded by the Korean government (MSIP) (No. 2012R1A3A2026417) and the third Stage of Brain Korea 21 Plus Project.

Notes and references

[1] Department of Materials Science and Engineering, Yonsei University, Seoul, 120-749, South Korea. E-mail : prohsh@yonsei.ac.kr

[2] Energy Materials Center, Korea Institute of Energy Research, 102 Gajeongro, Yuseonggu, Daejeon, 305-343, South Korea

[3] School of Chemistry, University of St.andrews, Fife,KY16 9ST,United Kingdom

† Footnotes should appear here. These might include comments relevant to but not central to the matter under discussion, limited experimental and spectral data, and crystallographic data.

Electronic Supplementary Information (ESI) available: [details of any supplementary information available should be included here]. See DOI: 10.1039/b000000x/

1. S. C. Singhal, Solid State Ionics, 2002, 152-153, 405-410.
2. C. Song, Catalysis Today, 2002, 77, 17-49.
3. R. J. Gorte, H. Kim and J. M. Vohs, Journal of Power Sources, 2002, 106, 10-15.
4. Y. Lin, Z. Zhan, J. Liu and S. A. Barnett, Solid State Ionics, 2005, 176, 1827-1835.
5. S. McIntosh and R. J. Gorte, Chemical Reviews, 2004, 104, 4845-4865.
6. C. M. Finnerty, N. J. Coe, R. H. Cunningham and R. M. Ormerod, Catalysis Today, 1998, 46, 137-145.
7. J. H. Koh, Y. S. Yoo, J. W. Park and H. C. Lim, Solid State Ionics, 2002, 149, 157-166.
8. J. B. Goodenough and Y. H. Huang, Journal of Power Sources, 2007, 173, 1-10.
9. H. Kim, C. Lu, W. L. Worrell, J. M. Vohs and R. J. Gorte, Journal of the Electrochemical Society, 2002, 149, A247-A250.
10. S. I. Lee, J. M. Vohs and R. J. Gorte, Journal of the Electrochemical Society, 2004, 151, A1319-A1323.
11. S. McIntosh, J. M. Vohs and R. J. Gorte, Electrochimica Acta, 2002, 47, 3815-3821.
12. J. W. Fergus, Solid State Ionics, 2006, 177, 1529-1541.
13. S. Tao and J. T. S. Irvine, Nature Materials, 2003, 2, 320-323.
14. T. H. Shin, S. Ida and T. Ishihara, Journal of the American Chemical Society, 2011, 133, 19399-19407.
15. J.-H. Myung, H.-J. Ko, J.-J. Lee, J.-H. Lee and S.-H. Hyun, International Journal of Hydrogen Energy, 2012, 37, 11351-11359.
16. T. Hibino, A. Hashimoto, M. Yano, M. Suzuki and M. Sano, Electrochimica acta, 2003, 48, 2531-2537.
17. V. Modafferi, G. Panzera, V. Baglio, F. Frusteri and P. Antonucci, Applied Catalysis A: General, 2008, 334, 1-9.
18. I. Gavrielatos, V. Drakopoulos and S. G. Neophytides, Journal of Catalysis, 2008, 259, 75-84.
19. C. Lu, W. Worrell, J. Vohs and R. Gorte, Journal of The Electrochemical Society, 2003, 150, A1357-A1359.
20. S. Jung, C. Lu, H. He, K. Ahn, R. J. Gorte and J. M. Vohs, Journal of Power Sources, 2006, 154, 42-50.
21. H. Ju, S. Uhm, J. W. Kim, R.-H. Song, H. Choi, S.H. Lee and J. Lee, Journal of Power Sources, 2012, 198, 36-41.
22. E. Nikolla, J. Schwank and S. Linic, Journal of Catalysis, 2009, 263, 220-227.
23. E. Nikolla, J. Schwank and S. Linic, Journal of catalysis, 2007, 250, 85-93.
24. E. Nikolla, A. Holewinski, J. Schwank and S. Linic, Journal of the American Chemical Society, 2006, 128, 11354-11355.
25. D. Simwonis, F. Tietz and D. Stöver, Solid State Ionics, 2000, 132, 241-251.
26. S. Zha, W. Rauch and M. Liu, Solid State Ionics, 2004, 166, 241-250.
27. S.D. Kim, H. Moon, S.H. Hyun, J. Moon, J. Kim and H.W. Lee, Journal of power sources, 2006, 163, 392-397.
28. S.D. Kim, H. Moon, S.H. Hyun, J. Moon, J. Kim and H.W. Lee, Solid State Ionics, 2006, 177, 931-938.
29. J.H. Myung, H. J. Ko, H.-G. Park, M. Hwan and S.H. Hyun, International Journal of Hydrogen Energy, 2012, 37, 498-504.
30. Z. Hou, O. Yokota, T. Tanaka and T. Yashima, Applied Surface Science, 2004, 233, 58-68.
31. C. A. Bateman, S. J. Bennison and M. P. Harmer, Journal of the American Ceramic Society, 1989, 72, 1241-1244.
32. J. W. Shabaker, G. W. Huber and J. A. Dumesic, Journal of Catalysis, 2004, 222, 180-191.

